PROCEEDINGS OF SCIENCE

MoEDAL: Expanding the LHC's Discovery Frontier

Michael Staelens[*†]
University of Alberta
E-mail: staelens@ualberta.ca

MoEDAL (Monopole and Exotics Detector at the LHC) is the 7^{th} experiment, specifically dedicated to investigating beyond the Standard Model scenarios by searching for highly ionizing particles, such as magnetic monopoles or massive pseudo-stable charged particles and multiply electrically charged particles as messengers of new physics. Sharing the same interaction point as the LHCb experiment, MoEDAL is complementary to the larger ATLAS and CMS experiments, thereby expanding the discovery reach of the LHC. This largely passive detector is comprised of the following subdetectors: A large array of Nuclear Track Detector (NTD) stacks, a magnetic trapping detector (designed to trap both electrically and magnetically charged highly ionizing particles), and a TimePix chip array that monitors particle backgrounds. The MoEDAL Apparatus for Penetrating Particles (MAPP), a new MoEDAL subdetector, is currently being designed and constructed, while the prototype deployed in 2017 is currently being analyzed. The aim of MAPP is to enable MoEDAL to search for fractionally charged particles as well as new long-lived neutrals. The goal of this poster presentation was to summarize the growing physics program of MoEDAL including MAPP's search for new fractionally charged particles, introduce the detectors and methodology, as well as present MoEDAL's latest results on magnetic monopole production at the LHC.

7th Annual Conference on Large Hadron Collider Physics - LHCP2019
20-25 May, 2019
Puebla, Mexico

[*]Speaker.
[†]On Behalf of the MoEDAL Collaboration

PoS(LHCP2019)031

1. Introduction

MoEDAL, the 7^{th} and newest experiment at the LHC, is dedicated to searching for highly ionizing particles as messengers of new physics [1]. MoEDAL's main motivation is to search for magnetic monopoles, however it can also search for any massive (pseudo-)stable, slow-moving particles with single or multiple eletric charges. These are found in many scenarios beyond the SM, and are described in detail in MoEDAL's physics program (see [2]). MoEDAL has taken data in 8 TeV and 13 TeV p-p collisions as well as in pb-pb collisions. The most recent results for 13 TeV p-p collisions will be summarized here.

Throughout the LHC's long shutdown, MoEDAL has been planning and constructing the MoEDAL Apparatus for Penetrating Particles (MAPP) detector, which we plan to install to take 30 fb^{-1} of data available at IP8 during LHC's RUN-3. The purpose of MAPP is to search for both minicharged particles (mCPs) and long-lived neutral particles (LLPs). To achieve this, MAPP will be composed of 2 active subdetectors: A roughly 150 m^3 LLP detector and a central 3 m^3 scintillation detector for mCP. This manuscript focuses strictly on the minicharge subdetector, MAPP-mCP, and its sensitivity to mCPs produced in Dark QED via the Drell-Yan process. Specifically, we show that the maximum reach of MAPP-mCP extends down to $\sim Q = 3e/1000$ for masses of $0.1 <$ M$_{mCP}$ $<$ 100 GeV.

The MAPP detector will be situated in the UGCI gallery adjacent to the MoEDAL/VELO region at IP8 shown in Figure 1. The generous dimensions of the UGCI gallery allow for decay zones of up to 10 m which also facilitate the search for new LLPs. The large sized cavern also enables MAPP to be positioned roughly 50 to 25 m away from IP8 (5° to 25°), where it is also shielded from SM collision products by at least 25 m of rock. Additionally, there is a ∼100 m overburden of rock, protecting MAPP from cosmic rays. The ability to place MAPP at a small angle to the beam (rather than a large angle) allows for a larger geometric acceptance for lower mass particles produced via the Drell-Yan process. When combined with the factor of 5 increase in luminosity planned for IP8 during Run-3, the larger luminosities enjoyed by the general purpose LHC experiments are largely eliminated for the new physics process benchmarked here. Thus, MAPP is expected to make a competitive and complementary contribution to the search for electric minicharge.

This paper will begin with a brief outline of the MoEDAL detector, followed by MoEDAL's latest results on magnetic monopole production at the LHC in p-p collisions with 13 TeV collision energy. For the first time at the LHC, this data was also interpreted considering photon-photon fusion as a possible production channel. Section 3 will discuss MAPP-mCP in detail. In section 4, MAPP's potential reach for mCPs (new Dirac fermions with Q $<<$ e) will be discussed. The final section concludes with future plans for MAPP alongside some closing remarks on the search for mCP.

2. The MoEDAL Detector

The MoEDAL detector is optimized to search for highly-ionizing particles, such as magnetic monopoles, dyons, highly electrically charged objects (HECOs), etc. This is achieved using 3 main

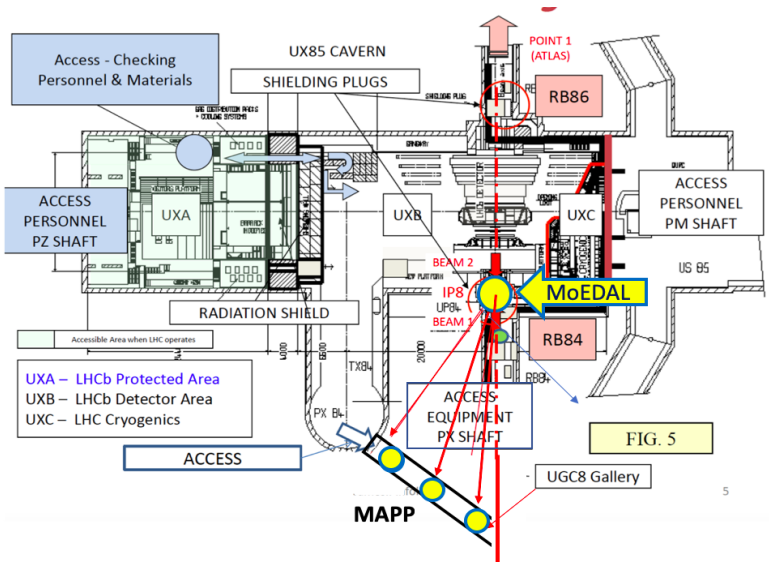

Figure 1: The possible positioning of the MAPP detector in UGCI.

subdetectors: A large Nuclear Track Detector (NTD) Array, a magnetic trapping detector, and an array of TimePix chips. A quick outline of the subdetectors and their underlying analyses will be presented here; refer to [3] for a full description of the detector design. MoEDAL is placed at IP8, covering a large geometric acceptance of 70%[1]. Our Geant4 model of the MoEDAL detector today is shown in Fig. 2.

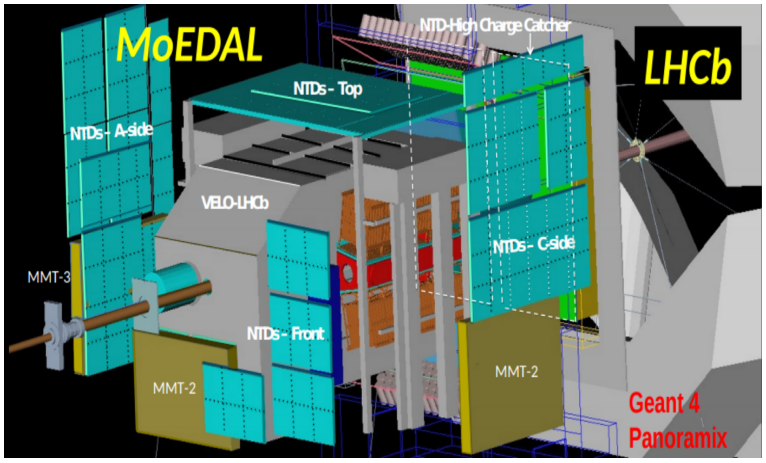

Figure 2: Modeling of the MoEDAL detector today using Geant4 Panoramix.

The MoEDAL detector is primarily a passive detector, with the exception being the TimePix chip array which actively monitors radiative backgrounds. The purpose of the NTD system is to

[1]This is to detect at least one Drell-Yan pair produced monopole.

track the ionization paths of highly ionizing particles that pass through the material, which also makes it insensitive to SM particles. In order to reveal the ionization paths, the NTD material is etched in a caustic NaOH solution. Using the heavy-ion beams at NA61 as well as the NASA Space Radiation Facility (NSRL), the NTD material stacks are calibrated, making MoEDAL uniquely optimized to searching for highly ionizing signatures of new physics. After etching, the material is scanned by human assisted computerized optical scanning microscopes searching specifically for the signature tracks caused by highly ionizing particles. In the future we intend to automate the scanning procedure using machine learning techniques. Using the NTD system alone, MoEDAL can place limits on various highly ionizing particle production channels. However, without the 794 kg of aluminum samples that form the magnetic trapping detector (MMT), MoEDAL would not be able to detect magnetic charge. This makes the MMT an indispensable addition to the NTD in the search for magnetic monopoles and dyons. The purpose of the MMT volumes is to slow down and trap magnetically charged particles that ionize as they pass through it. The choice of aluminum is due to the nucleus having a large, positive anomalous magnetic moment which facilitates monopole trapping. The aluminum samples exposed to the p-p collisions are also removed for analysis, which involves passing the samples through a Superconducting QUantum Interference Device (SQuID) magnetometer at ETH Zurich. The clear signal for magnetic charge would be a sharp rise in the current through the superconducting loop (as the magnetically charged particles passes through the superconducting magnetometer) which then remains constant. This would be analogous to simply running a single N or a S pole of a magnet through the SQuID.

MoEDAL's latest results on magnetic monopole production at the LHC make use of the MMT subdetector which was exposed to 4.0 fb^{-1} of 13 TeV proton-proton collisions at IP8. In the subsequent analysis performed, MoEDAL considered monopoles with spins 0, 1/2, and 1, as well as assuming both β-dependent and -independent couplings. For the first time at the LHC, this data was also interpreted including $\gamma\gamma$-fusion as a possible production mechanism, rather than only the usual Drell-Yan-like mechanism considered. The Feynman-like diagrams for these channels are shown in Fig. 3. From this search, MoEDAL excludes magnetic charges of $g > g_D = 68.5e$ in all samples and as a result, provides the best current limits on labratory produced magnetic monopoles with $2g_D < g < 5g_D$ and masses up to 2 TeV, as shown in Fig. 4. ATLAS's latest results are also shown here, which now mark the best limits for a magnetic charge of 1 g_D. For the full paper on MoEDAL's latest results see [4].

3. MoEDAL's MAPP-mCP Subdetector

As previously mentioned, this paper focuses only on the central core of the MAPP detector which is designed to search for minicharged particles (MAPP-mCP). The compact central section of MAPP that forms MAPP-mcP is made of two colinear sections, each with a cross-sectional area of 1 m^2 and comprising 100 (10 x 10 cm) plastic scintillator sections. Both of these are 1.5 m long and sub-divided into two 75 cm bars. Thus, a through-going particle from the IP will encounter 3

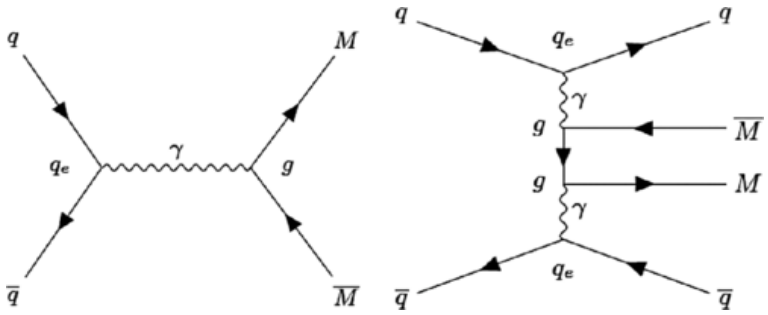

Figure 3: Feynman-like diagrams for direct production of monopole pairs at leading order via the Drell-Yan (left) and $\gamma\gamma$-fusion (right) processes at the LHC. A four-vertex diagram is also included for scalar and vector monopoles.

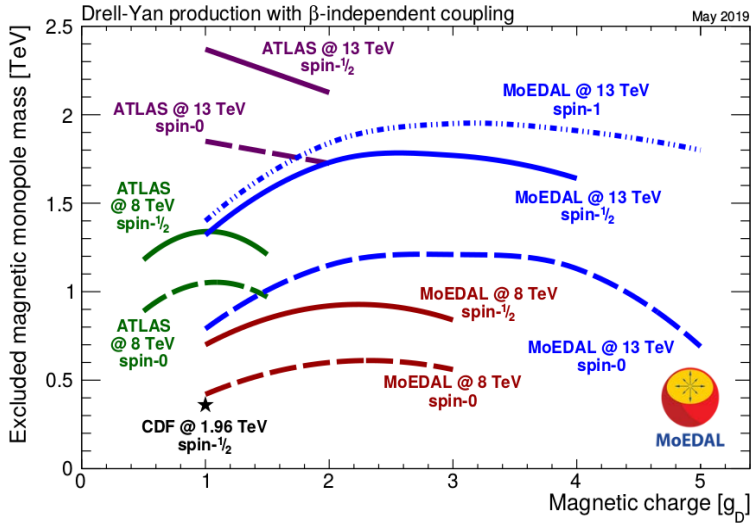

Figure 4: Excluded magnetic monopole masses for pair produced monopoles at collider experiments, with MoEDAL's latest results shown in blue (using β-independent couplings).

m (4 x 75 cm) of scintillator. The 4 scintillator bars are each readout by a single PMT, with all four PMTs placed in coincidence in order to essentially eliminate backgrounds from dark counts in the PMTs and radiogenic signals in the plastic scintillator or PMTs. Figure 5 shows a sketch of one of the four 75 cm long sections. The detectors are protected from cosmic rays and from particle interactions in the surrounding rock by charged particle veto detectors. A sketch of the detector in the tunnel is given in Figure 6. The scintillator used by MAPP-mCP is developed by MoEDAL's IEAP group to have enhanced light output.

The nested system of three detectors that surrounds the MAPP-mCP detector, forms the MAPP-Long Lived Particle (LLP) detector. Each detector system is formed of 5 faces butted against the

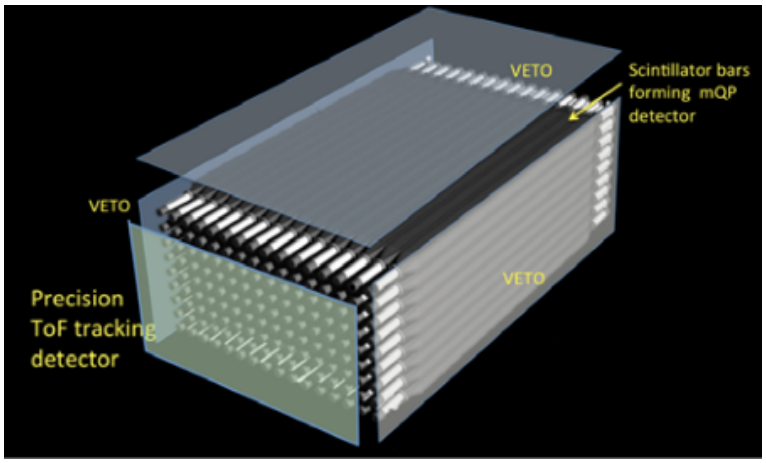

Figure 5: A sketch of one of the four subunits of MAPP-mCP.

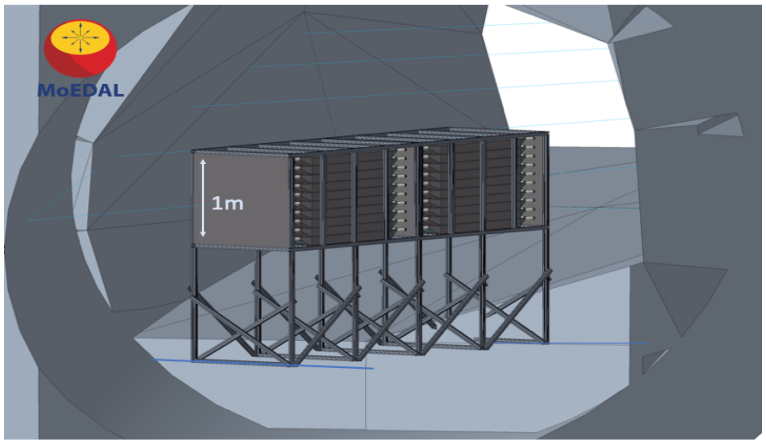

Figure 6: A sketch of the MAPP-mCP subdetector (1 m^2 x 3 m).

forward veto plane, which forms the sixth face. Each face is comprised of scintillator strips arranged in an x/y configuration, readout by SiPMs, allowing position and ToF determination. The outer layer of the MAPP-LLP detector borders the acceptance region of the MAPP-LLP system. The MAPP-LLP detector system also acts as a charged particle veto for the MAPP-mCP detector. In addition, the MAPP-mCP detector is sandwiched between 3 $1m^2$ detector veto planes as further protection against charged particles crossing the MAPP-mCP detector. The baseline technology of the large ToF planes is plastic scintillator. But other detector technologies such as MRPCs would also be very appropriate and could be expected to give a better position and ToF resolution. The protected environment of the UGCI gallery provides a low radiation background situation for the MAPP detector.

In the case of the minicharged detector we expect to have sensitivity to electric charges from 10^{-1} e to 10^{-3} e for masses in the range 0.1 to 100 GeV. The energy deposited per unit length (dE/dx) by fractionally charged particles is proportional to the square of the charge. Thus, a particle with a charge as low as 10^{-3} e would have a dE/dx a millionth that of singly charged

relativistic particle. Therefore. the MAPP-mCP detector should present a large path length of scintillator to the impinging particle in order to produce a measurable signal which can be as small as one photo-electron produced in the PMT. In order to study the response of the planned MAPP detector a prototype was deployed for data taking late in 2017 and is still currently under study. A photograph of this deployment is shown Figure 7. Aside from testing the feasibility of MAPP-mCP, the prototype will also assist in understanding the backgrounds expected by MAPP-mCP. Using this data we can further optimize the detector before deploying in RUN-3.

Figure 7: A photograph of the small MAPP-mCP prototype deployed at UX85.

4. The Search for Fractional Charge at MAPP

Particles with an electric charge much smaller than the electric charge e, have been discussed in connection with the mechanism of electric charge quantization and possible non-conservation of electric charge [5]. The existence of mCPs has also been proposed in various extensions of the Standard Model (SM). In particular, in the hidden (dark) sector models with a new $U'(1)$ gauge group [6].

We explore the possibility of detecting such particles with MAPP-mCP, using an example a scenario in which a new massless $U'(1)$ gauge field, the dark-photon (A') is coupled to the SM hypercharge field. A new massive dark-fermion (ψ) of mass M_{mCP}, is also predicted. This dark-fermion is charged under the new U(1) field A' with charge e'. The Lagrangian for the model is given by,

$$\mathscr{L} = \mathscr{L}_{SM} - \frac{1}{4}A'_{\mu\nu}A'^{\mu\nu} + i\bar{\psi}(\partial\!\!\!/ + ie'A\!\!\!/' + iM_{mCP})\psi - \frac{\kappa}{2}A'_{\mu\nu}B^{\mu\nu}. \tag{4.1}$$

The last term depicts the kinetic mixing between A' and the hypercharge field B. We can eliminate the mixing term by expressing the new gauge boson as, $A'_\mu \Rightarrow A'_\mu + \kappa B_\mu$. This simple field redefinition reveals a coupling between the charged matter field ψ to hypercharge. The Lagrangian shown above then becomes:

$$\mathscr{L} = \mathscr{L}_{SM} - \frac{1}{4}A'_{\mu\nu}A'^{\mu\nu} + i\bar{\psi}(\partial\!\!\!/ + ie'A\!\!\!/' - i\kappa e'B\!\!\!/ + iM_{mCP})\psi. \tag{4.2}$$

Thus, the field ψ therefore acts as a field charged under hypercharge with a minicharge (mCP) $\kappa e'$. The new minicharged matter field ψ couples to the photon and Z^0 boson with a charge $\kappa e' \cos\theta_W$ and $\kappa e' \sin\theta_W$, respectively. The fractional charge in terms of electric charge is thus $\varepsilon = \kappa e' cos\theta_W / e$.

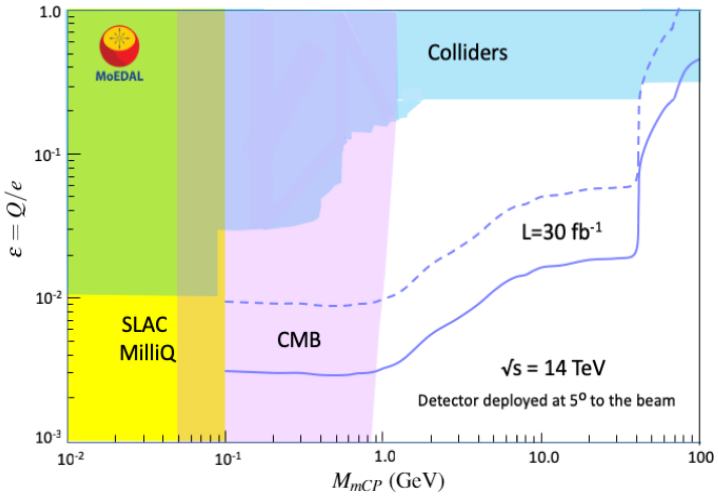

Figure 8: The maximum reach of the MAPP detector using 30 fb^{-1} of data in LHC's RUN-3. The solid line represents that points at which 3 events would be observed assuming 100% efficiency and no background. The dotted line represents the case where 3 events are observed with an overall signal detection efficiency of 10%.

The most stringent strongest direct limits on mCPs for 10^{-1} to 10^{-5} for $M_{mCP} < 300$ GeV have been derived from accelerator-based searches [7][8]. Indeed, the inspiration for MAPP came from the one such dedicated direct search for mCPs at SLAC [7]. Another, experiment, milliQan [9], dedicated to the search for mCP at the LHC, is planned for LHC's Run-3. This detector will be deployed at 45° to the beam roughly 30m away from the CMS detector. In addition, there are a number of indirect searches for mCP using astrophysical systems [10-12]. Even if we take the astrophysical bounds at face value and combine them with direct searches, most of the parameter space for mCPs with masses $0.1 \leq M_{mCP} < 100$ GeV, is unexplored, as shown in Figure 8.

In order to establish the potential of detecting minicharged particles at the LHC with MoEDAL's MAPP-mCP subdetector, we implemented the model presented here into Madgraph5 [13] using Feynrules and Mathematica. This model was validated by performing several comparisons with the literature available. Using the validated model we generated events at $\sqrt{s} = 14$ TeV and assuming an integrated luminosity of 30 fb^{-1}, for various values of M_{mCP} and ε. These events were then passed to an in-house script which simulates MAPP-mCP. Requiring a minimum of 3 mCP tracks through the detector, we determine MAPP-mCP's expected 95% confidence limit assuming

overall detector efficiencies of 100% and 10%. The maximum possible reach for the detector using this data is indicated in Figure 8, demonstrating MAPP-mCP's coverage of a significant portion of the free parameter space. These bounds could be further improved by including ψ couplings to the psion and Υ resonances. With the factor of 10 increase in luminosity expected during HL-LHC, MAPP can make further contributions to the search for minicharge.

5. Conclusion

In this article, MoEDAL's latest results were summarized alongside a brief exposition of MoEDAL's future plans to search for mCPs during LHC RUN-3 with the new MAPP-mCP subdetector. We expect that the planned detector should make a competitive contribution to the search for mCP at the LHC. This study is currently being extended to include more mCP scenarios, several LLP channels, and a full Geant4 simulation of the detector which also includes the material between MAPP and IP8. A comprehensive study of the backgrounds expected at MAPP is also underway.

References

[1] http://moedal.web.cern.ch/

[2] B. Acharya, et. al. [MoEDAL Collaboration], *The Physics Programme Of The MoEDAL Experiment At The LHC*, *Int. J. Mod. Phys. A* 29 (2014) 1430050.

[3] S. Cecchini, et. al. [MoEDAL Collaboration (2009)], *Technical Design Report of the MoEDAL Experiment*, CERN Preprint CERNLHC-2009-006, MoEDAL-TDR-1.1 [hep-ph/1405.7662]

[4] B. Acharya, et. al. [MoEDAL Collaboration], *Magnetic monopole search with the full MoEDAL trapping detector in 13 TeV pp collisions interpreted in photon-fusion and Drell-Yan production*, *PRL* 123 (2019 021802 [hep-ph/1903.08491].

[5] A.Yu. Ignatiev, V.A. Kuzmin, M.E. Shaposhnikov, *Is The Electric Charge Conserved?*, *Phys. Lett. B* 84 (1979) 315.

[6] B. Holdom, *Two U(1)'s and Epsilon Charge Shifts*, *Phys. Lett. B* 166 (1986) 196.

[7] A. Prinz, R. Baggs, J. Ballam, S. Ecklund, C. Fertig, et al., *Search for Millicharged Particles at SLAC*, *PRL* 81 (1998) 1175 [hep-ex/9804008].

[8] S. Chatrchyan, et al. [CMS Collaboration], *Search for fractionally charged particles in pp collisions at sqrt(s) = 7 TeV*, *Phys. Rev. D* 87 (2013) 092008 [hep-ph/1210.2311].

[9] A. Haas, C. Hill, E. Izaguirre and I. Yavin, *Looking for milli-charged particles with a new experiment at the LHC*, *Phys. Lett. B* 746 (2015) 117 [hep-ph/1410.6816].

[10] S. Davidson, S. Hannestad, G. Raffelt, *Updated Bounds on Milli-Charged Particles*, *JHEP* 0005 (2000) 003 [hep-ph/0001179].

[11] S. Davidson, M.E. Peskin, *Astrophysical Bounds on Milli-Charged Particles in Models with a Paraphoton*. *Phys. Rev. D* 49 (1994) 2114 [hep-ph/9310288].

[12] S.L. Dubovsky, D. S. Gorbunov, G. I. Rubtsov, *Narrowing the window for millicharged particles by CMB anisotropy*, *JETP Letters* 79 (2004) 1 [hep-ph/0311189].

[13] J. Alwall, et. al., *The Automated Computation of Tree-level and Next-to-Leading Order Differential Cross Sections, and Their Matching to Parton Shower Simulations*, [hep-ph/1405.0301].